

Enhancement of the stability of resistive switching characteristics by conduction path reconstruction

Jheng-Jie Huang, Ting-Chang Chang, Chih-Cheng Yu, Hui-Chun Huang, Yu-Ting Chen, Hsueh-Chih Tseng, Jyun-Bao Yang, Simon M. Sze, Der-Shin Gan, Ann-Kuo Chu, Jian-Yang Lin, and Ming-Jinn Tsai

Citation: *Applied Physics Letters* **103**, 042902 (2013); doi: 10.1063/1.4816269

View online: <http://dx.doi.org/10.1063/1.4816269>

View Table of Contents: <http://scitation.aip.org/content/aip/journal/apl/103/4?ver=pdfcov>

Published by the [AIP Publishing](#)

Articles you may be interested in

[Resistive switching characteristics in dielectric/ferroelectric composite devices improved by post-thermal annealing at relatively low temperature](#)

Appl. Phys. Lett. **104**, 092903 (2014); 10.1063/1.4867260

[Multilevel recording in Bi-deficient Pt/BFO/SRO heterostructures based on ferroelectric resistive switching targeting high-density information storage in nonvolatile memories](#)

Appl. Phys. Lett. **103**, 263502 (2013); 10.1063/1.4855155

[Multi-state resistive switching memory with secure information storage in Au/BiFe_{0.95}Mn_{0.05}O₃/La_{5/8}Ca_{3/8}MnO₃ heterostructure](#)

Appl. Phys. Lett. **100**, 193504 (2012); 10.1063/1.4714514

[Structural, electrical, and magnetic properties of chemical solution deposited BiFe_{1-x}Ti_xO₃ and BiFe_{0.9}Ti_{0.05}Co_{0.05}O₃ thin films](#)

J. Appl. Phys. **106**, 014103 (2009); 10.1063/1.3158556

[Degradation of ferroelectric properties in integrated Pt/SrBi₂Ta₂O₉/Pt capacitor by impurity diffusion from interlevel dielectric layer](#)

Appl. Phys. Lett. **81**, 4230 (2002); 10.1063/1.1525060



NEW! Asylum Research MFP-3D Infinity™ AFM
Unmatched Performance, Versatility and Support

OXFORD INSTRUMENTS
The Business of Science®

Stunning high performance
Simpler than ever to GetStarted™
Comprehensive tools for nanomechanics
Widest range of accessories for materials science and bioscience

The advertisement features several images: a blue textured surface, a brown textured surface, a grid of colorful rectangular samples, and the Asylum Research MFP-3D Infinity AFM instrument.

Enhancement of the stability of resistive switching characteristics by conduction path reconstruction

Jheng-Jie Huang,¹ Ting-Chang Chang,^{1,2,3,a)} Chih-Cheng Yu,⁴ Hui-Chun Huang,⁵ Yu-Ting Chen,² Hsueh-Chih Tseng,¹ Jyun-Bao Yang,² Simon M. Sze,^{1,6} Der-Shin Gan,⁵ Ann-Kuo Chu,² Jian-Yang Lin,⁷ and Ming-Jinn Tsai⁸

¹Department of Physics, National Sun Yat-Sen University, Kaohsiung 804, Taiwan

²Department of Photonics, National Sun Yat-Sen University, Kaohsiung, Taiwan

³Advanced Optoelectronics Technology Center, National Cheng Kung University, Tainan 701, Taiwan

⁴Graduate School of Opto-Electronics, National Yunlin University of Science and Technology, Yunlin 640, Taiwan

⁵Department of Materials and Optoelectronic Science, National Sun Yat-Sen University, Kaohsiung 804, Taiwan

⁶Department of Electronics Engineering, National Chiao Tung University, Hsinchu 300, Taiwan

⁷Department of Electronic Engineering, National Yunlin University of Science and Technology, Yunlin 640, Taiwan

⁸Electronics and Optoelectronics Research Laboratory, Industrial Technology Research Institute, Chutung, Hsinchu 310, Taiwan

(Received 27 May 2013; accepted 5 July 2013; published online 23 July 2013)

In this study, a Pt/BiFeO₃/TiN device was fabricated and the resistance switching characteristics were investigated. After the first forming process, the conduction path was formed and exhibited unstable bipolar switching characteristics. Subsequently, the original conduction path was destroyed thoroughly by high negative bias. By reconstructing the conduction path after a second forming process (re-forming process), the device exhibits stable bipolar switching characteristics. Transmission electron microscopy analysis indicates that the stability of switching behavior was enhanced because of the joule heating effect, and is an easy way to improve the resistance switching characteristics. © 2013 AIP Publishing LLC. [<http://dx.doi.org/10.1063/1.4816269>]

With the development of portable electronic products, the thin film transistor for display^{1,2,16,17} and nonvolatile memory for storage has been widely utilized.³ However, traditional nonvolatile floating gate memory device has confronted some physical limits as devices continuously scaled down,^{3,18,19} and resistance random access memory (RRAM) is considered one of the best potential candidates for development of the next generation of nonvolatile memory because of advantages such as low operating power consumption, high density due to simple device structure, and a fast switching speed of about several ns.^{4,5} A number of materials have been investigated for their resistive switching characteristics, such as HfO₂, ZnO, and InGaZnO.^{4,6–10} Information can be stored in the RRAM devices by the various resistance states,⁴ and therefore resistive switching property is very important. Hence, ways of enhancing the resistance switching characteristics have been proposed. For example, a thermal process has been used to anneal the resistive switching layer, enhancing the resistive switching property.¹⁰ However, the fabrication of a RRAM device is a back-end-of-line (BEOL) process, and the material property of the TiN bottom electrode might be affected by the thermal process.

BiFeO₃ (BFO) is a multiferroic material which has been applied to ferroelectric random-access memory¹¹ and magnetoresistive random-access memory¹² devices because of its ferroelectricity. Additionally, the resistive switching characteristics of BiFeO₃ have been investigated. In this letter,

we employ BFO as the resistive switching layer because BFO film exhibits special characteristics that can enhance the stability of resistive switching characteristics.

The proposed RRAM device was fabricated on a TiN/SiO₂/Si substrate. We deposited the 25 nm-thick BFO film as a resistance switching layer by RF sputtering a BiFeO₃ target in Ar (30 sccm) ambient at room temperature. Subsequently, we sputtered 100 nm-thick Pt on the BFO film as the top electrode, completing the RRAM device as a Pt/BFO/TiN structure. We investigated the resistive switching properties and measured the I-V curves with an Agilent B1500 semiconductor parameter analyzer and the structural characteristics were investigated by transmission electron microscopy (TEM, FEI Tecnai G2 F20).

During the measurement process, the bias was applied on the TiN electrode and the Pt electrode was ground, as shown in Fig. 1(a). Figure 1(b) shows the forming process necessary to produce a conduction path. After the first forming process, the conduction path is formed, and the resistance value can be switched repeatedly by applying positive or negative voltage, as shown in Fig. 1(c). During the forming process, the electrons receive sufficient energy to break the metal-oxygen bonds, and the oxygen will migrate to the TiN because of the electric field direction. As negative bias is applied, the oxygen ion will oxidize the conduction path near the TiN bottom electrode, and the conduction path will rupture.^{13,14} Subsequently, the positive voltage can break the metal-oxygen bond again, and the conduction path near the TiN electrode is re-formed. The ruptured conduction path is defined as high resistance state (HRS) and the unbroken

^{a)}Author to whom correspondence should be addressed. Electronic mail: tcchang@mail.phys.nsysu.edu.tw.

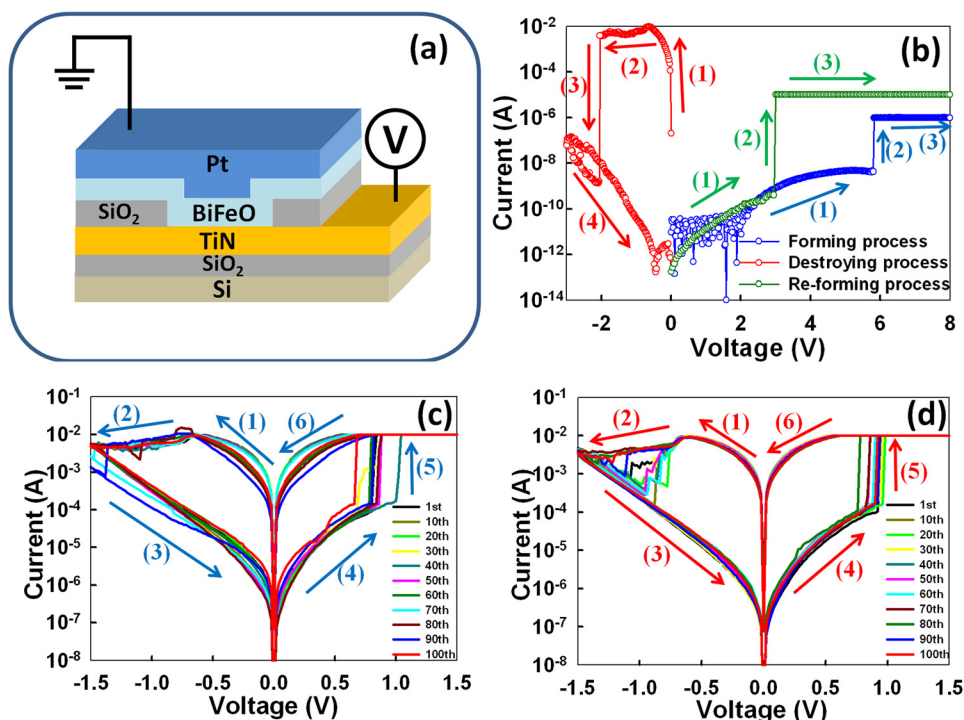


FIG. 1. (a) Structure of BiFeO₃ based RRAM device. (b) I-V curves of forming and re-forming process. Resistive switching characteristics of BiFeO₃ after (c) forming process and (d) after re-forming process.

conduction path is defined as low resistance state (LRS). Subsequently, a higher negative bias sweeping from 0 V to -2.5 V was applied to destroy the original conduction path thoroughly, as shown with the red line in Fig. 1(b), and the conduction path is reconstructed by second forming process (re-forming process). Figure 1(d) shows the resistance switching characteristics after the re-forming process. A comparison of Figures 1(c) and 1(d) clearly shows the resistive switching behavior after the re-forming process is more stable than the initial resistive switching characteristics (after the forming process).

In order to investigate the change of BFO resistance switching layer before and after the higher negative bias sweeping, we analyzed the structure by TEM images. Figure 2(a) shows the TEM image of the Pt/BiFeO₃/TiN structure which has undergone the first forming process and one hundred DC cycle sweeps, with the BFO layer in an amorphous state. After the higher negative bias sweeping and re-forming process, the BFO film will crystallize, as shown in Fig. 2(b). This phenomenon indicates that the higher negative bias sweeping or re-forming process provides large thermal energy and the stability of resistive switching behavior is enhanced by the thermal effect.

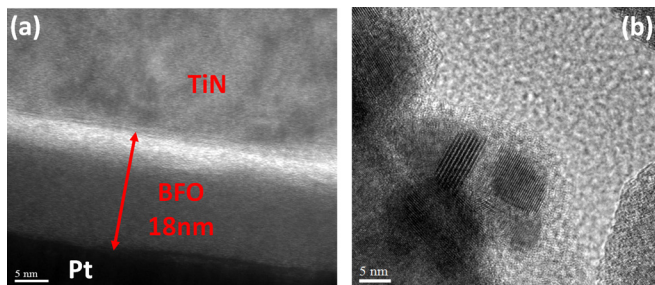


FIG. 2. TEM images of BFO film after (a) forming process and (b) re-forming process.

From the equation of the joule heating effect, P (power) = I (current) \times V (voltage), the large thermal energy can be supplied during the reset process with the higher negative bias sweeping. From these results, the switching mechanism of BFO film can be proposed. At the initial state, there are many defects in the BFO film, as shown in Fig. 3(a). In order to form the conduction path, a higher positive voltage is applied and the electrons receive sufficient energy to break the metal-oxygen bond. After the metal-oxygen bond is broken, the oxygen ions migrate to the TiN electron and the conduction filament (or path) is formed along defects, as shown in Fig. 3(b). As the higher negative bias is applied, the joule heating effect supplies large thermal energy and anneals the area near the filament, as shown in Fig. 3(c). Because of the localized thermal effect, the area surrounding the filament crystallizes. Hence, the defects can be reduced and the conduction path will be thoroughly destroyed, as shown in Fig. 3(d). Subsequently, the conduction path can be reconstructed by the re-forming process.

In order to investigate the difference in resistive switching characteristics after the forming process and after the re-forming process, we extracted the resistance value of LRS and HRS by DC sweep cycles at 0.2 V, as shown in Figs. 4(a) and 4(b). According to the LRS/HRS statistics, the on/off ratio after forming process is unstable because the defect affects the migration of oxygen ions during the set/reset process. Figures 4(c) and 4(d) shows set voltage (V_{set}) and reset voltage (V_{reset}), with the variation of V_{set} and V_{reset} decreasing after the re-forming process. This is because the conduction path is dominated by the quantity of defects in the resistance switching layer. The more defects which exist, the more conduction paths which will form during each set/reset cycle.¹⁵

In summary, because the fabrication of RRAM device is a back-end-of-line (BEOL) process, it is difficult to anneal by a thermal process, so we propose a simple way to enhance

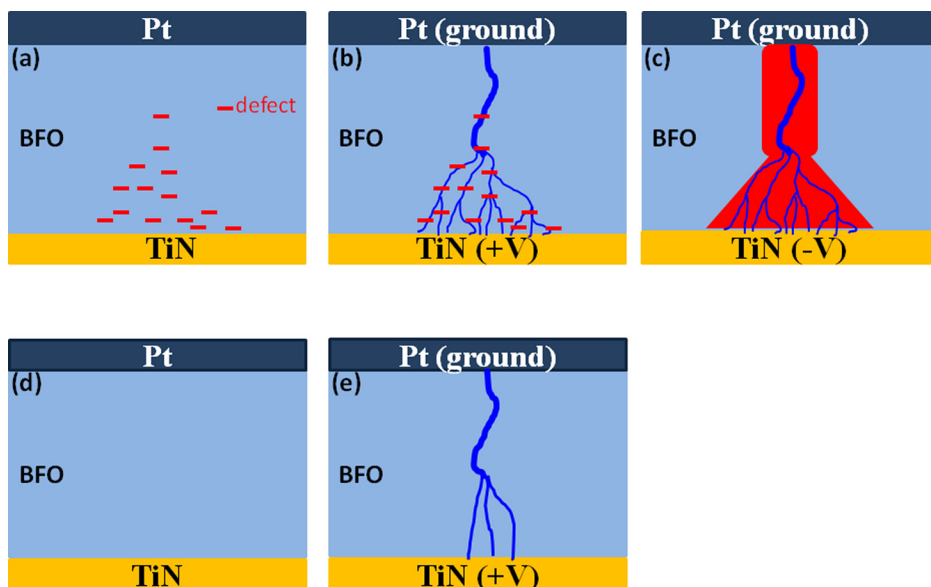


FIG. 3. Diagram of (a) initial state, (b) formation of conduction path, (c) annealing process, (d) the destroyed conduction path, and (e) the conduction path reconstruction.

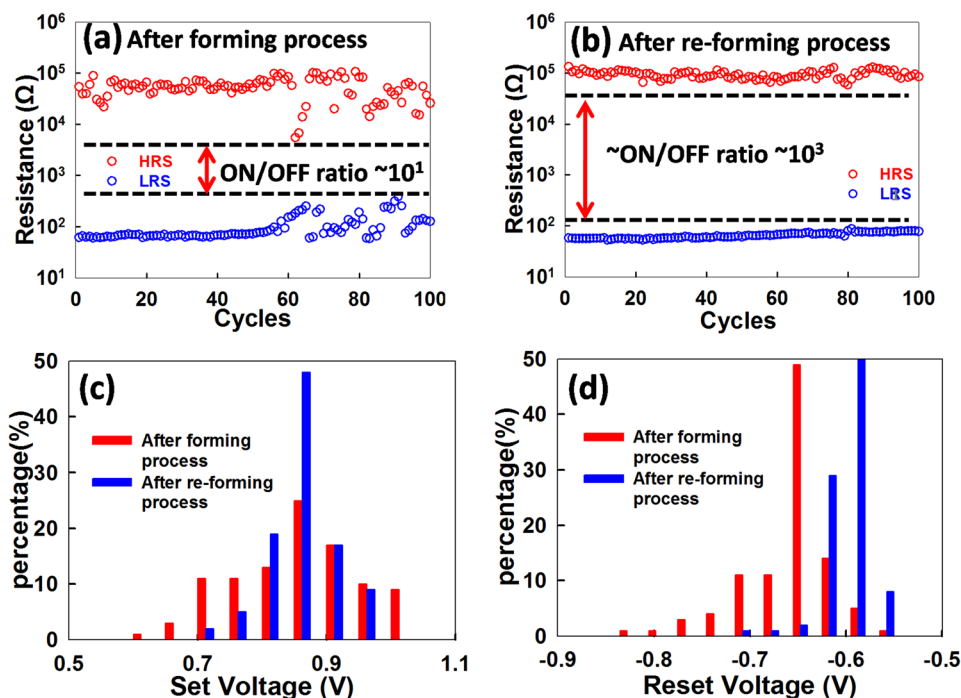


FIG. 4. HRS/LRS statistics of switching characteristics (a) after forming process and (b) after re-forming process. (c) Set voltage and (d) reset voltage statistics.

the stability of such a nonvolatile resistance switching memory device. After a high negative bias stress, the BiFeO₃ film will be annealed by the joule heating effect and will crystallize. Hence, the quantity of defects in the BiFeO₃ film can be reduced, and the stability of resistive switching characteristic can be enhanced.

This work was performed at National Science Council Core Facilities Laboratory for Nano-Science and Nano-Technology in Kaohsiung-Pingtung area, NSYSU Center for Nanoscience and Nanotechnology, and was supported by the National Science Council of the Republic of China under Contract Nos. NSC-102-2120-M-110-001.

¹C. T. Tsai, T. C. Chang, S. C. Chen, I. Lo, S. W. Tsao, M. C. Hung, J. J. Chang, C. Y. Wu, and C. Y. Huang, *Appl. Phys. Lett.* **96**, 242105 (2010).

²T. C. Chen, T. C. Chang, C. T. Tsai, T. Y. Hsieh, S. C. Chen, C. S. Lin, M. C. Hung, C. H. Tu, J. J. Chang, and P. L. Chen, *Appl. Phys. Lett.* **97**, 112104 (2010).

³T. C. Chang, F. Y. Jian, S. C. Chen, and Y. T. Tsai, *Mater. Today* **14**(12), 608 (2011).

⁴S. S. Sheu, P. C. Chiang, W. P. Lin, H. Y. Lee, P. S. Chen, Y. S. Chen, T. Y. Wu, Frederick T. Chen, K. L. Su, M. J. Kao, K. H. Cheng, and M. J. Tsai, in *VLSI Circuits Dig.*, (2009), pp. 82–83.

⁵W. C. Chien, F. M. Lee, Y. Y. Lin, M. H. Lee, S. H. Chen, C. C. Hsieh, E. K. Lai, H. H. Hui, Y. K. Huang, C. C. Yu, C. F. Chen, H. L. Lung, K. Y. Hsieh, and C.-Y. Lu, in *VLSI Tech. Symp.*, (2012), pp. 153–154.

⁶S. Yu, B. Gao, H. Dai, B. Sun, L. Liu, X. Liu, R. Han, J. Kang, and B. Yu, *Electrochem. Solid-State Lett.* **13**, H36 (2010).

⁷K. L. Lin, T. H. Hou, J. Shieh, J. H. Lin, C. T. Chou, and Y. J. Lee, *J. Appl. Phys.* **109**, 084104 (2011).

⁸W. Y. Chang, Y. C. Lai, T. B. Wu, S. F. Wang, F. Chen, and M. J. Tsai, *Appl. Phys. Lett.* **92**, 022110 (2008).

⁹M. C. Chen, T. C. Chang, C. T. Tsai, S. Y. Huang, S. C. Chen, C. W. Hu, S. M. Sze, and M. J. Tsai, *Appl. Phys. Lett.* **96**, 262110 (2010).

¹⁰S. Kim, H. Moon, D. Gupta, S. Yoo, and Y. K. Choi, *IEEE Trans. Electron Devices* **56**, 696 (2009).

¹¹Y. W. Chiang and J. M. Wu, *Appl. Phys. Lett.* **91**, 142103 (2007).

¹²J. Allibe, I. C. Infante, S. Fusil, K. Bouzouane, E. Jacquet, C. Deranlot, M. Bibes, and A. Barthélémy, *Appl. Phys. Lett.* **95**, 182503 (2009).

- ¹³Y. E. Syu, T. C. Chang, T. M. Tsai, Y. C. Hung, K. C. Chang, M. J. Tsai, M. J. Kao, and S. M. Sze, *IEEE Electron Device Lett.* **32**(4), 545–547 (2011).
- ¹⁴Y. T. Chen, T. C. Chang, P. C. Yang, J. J. Huang, H. C. Tseng, H. C. Huang, J. B. Yang, A. K. Chu, D. S. Gan, M. J. Tsai, and S. M. Sze, *IEEE Electron Device Lett.* **34**, 226 (2013).
- ¹⁵J. J. Huang, T. C. Chang, J. B. Yang, S. C. Chen, P. C. Yang, Y. T. Chen, H. C. Tseng, Simon M. Sze, A. K. Chu, and M. J. Tsai, *IEEE Electron Device Lett.* **33**, 1387 (2012).
- ¹⁶M. C. Chen, T. C. Chang, S. Y. Huang, K. C. Chang, H. W. Li, S. C. Chen, J. Lu, and Y. Shi, *Appl. Phys. Lett.* **94**, 162111 (2009).
- ¹⁷Y. C. Chen, T. C. Chang, H. W. Li, S. C. Chen, J. Lu, W. F. Chung, Y. H. Tai, and T. Y. Tseng, *Appl. Phys. Lett.* **96**, 262104 (2010).
- ¹⁸S. C. Chen, T. C. Chang, P. T. Liu, Y. C. Wu, P. S. Lin, B. H. Tseng, J. H. Shy, S. M. Sze, C. Y. Chang, and C. H. Lien, *IEEE Electron Device Lett.* **28**, 809 (2007).
- ¹⁹W. R. Chen, T. C. Chang, J. L. Yeh, S. M. Sze, and C. Y. Chang, *Appl. Phys. Lett.* **92**, 152114 (2008).